PERGAMON

International Journal of Multiphase Flow 28 (2002) 1235–1247

International Journal of Multiphase Flow

www.elsevier.com/locate/ijmulflow

Brief communication

Gas–liquid two-phase flow in micro-channels

W.L. Chen, M.C. Twu, C. Pan *

Department of Engineering and System Science, National Tsing Hua University, 101, Sect 2, Kuang Fu Road, Hsinchu 30043, Taiwan, ROC

Received 2 August 2001; received in revised form 27 February 2002

1. Introduction

The two-phase flow in micro-channels is of fundamental importance for many interesting applications, such as cooling of micro-electronic components and devices by a compact heat exchanger, material processing and thin film deposition technology, bioengineering and biotechnology (Peng and Wang, 1993). Recently, there have been several studies on two-phase flow or boiling heat transfer in micro-channels. For example, Fukano and Kariyasaki (1993), Mishima and Hibiki (1996), Coleman and Garimella (1999), Tripplett et al. (1999a,b) and Xu et al. (1999) have studied two-phase flow pattern, bubble speed and/or pressure drop of air/water two-phase flows in circular or rectangular channels with their sizes in the order of 1 mm. For air/water at atmospheric pressure, the channels with the order of 1 mm may be considered as the micro-channels. This channel size is smaller than that evaluated from the Laplace constant, i.e., $(\sigma/(g(\rho_L - \rho_G)))^{1/2}$, where σ is the surface tension, ρ_L and ρ_G are the liquid and gas density, respectively, and g is the gravitational constant (Tripplett et al., 1999a,b). The Laplace constant for air/water two-phase flow at atmospheric pressure and room temperature conditions is 2.73 mm.

Thulasidas et al. (1995) examined the bubble diameter, liquid film thickness and the bubble speed in capillaries with circular and square cross-sections. The bubble diameter and the thickness of the thin liquid film between the bubble and the channel wall are of significant interest in predicting the heat and mass transfer rates between the fluid and the wall. On the other hand, Peng and Wang (1993), Aligoodarz et al. (1998), Zhang et al. (2000) and Lin et al. (2001) have explored flow boiling in micro-channels. Kennedy et al. (2000) investigated experimentally the onset of the flow boiling instability in micro-channels. Although the experimental works in the literature have reported many unique phenomena in small- and micro-channels, there is still no

* Corresponding author. Tel.: +886-3-572-5363/574-2662; fax: +886-3-572-0724.
E-mail address: cpan@ess.nthu.edu.tw (C. Pan).

PII: S0301-9322(02)00023-X

general theory available. Many works are still needed to explore the transport phenomena of two-phase flow in micro-channels.

The present study investigates experimentally the characteristics of nitrogen–water two-phase flows in glass micro-channels. The two-phase flow pattern, bubble speed and void fraction in the micro-channels were observed and analyzed through visualization. Two-phase flow pattern maps were constructed and correlations for bubble velocity and void fraction were proposed.

2. Experimental details

A schematic diagram of the experimental loop is illustrated in Fig. 1. The test section is a transparent glass capillary with a length of 510 mm. The gas–liquid two-phase flows in micro-channels with two different inner diameters, 1 and 1.5 mm, respectively, were investigated. The capillary inlet was enlarged to fit an injection needle head, a side tube and a pressure tap. The injection needle with its tip been cut flat, was used as the gas inlet. Nitrogen gas from a high-pressure tank enters the channel through the needle. Its flow rate was controlled and measured by a rotameter. On the other hand, water from the storage tank was forced into the channel through the side tube by the high-pressure nitrogen. The water flow rate was controlled and measured also by a rotameter. The water flow rate can be independently confirmed by weighing the water collected for a certain period of time. The measurement uncertainties of nitrogen and water superficial velocities were estimated to be ± 0.087 and ± 0.041 m/s, respectively.

Two-phase flow patterns in the channel were visualized by using a high-speed digital camera. For the best visualization, a light source was placed in front of the camera but behind the channel. Moreover, the light source was covered with a light red paper to reduce loss of the light due to

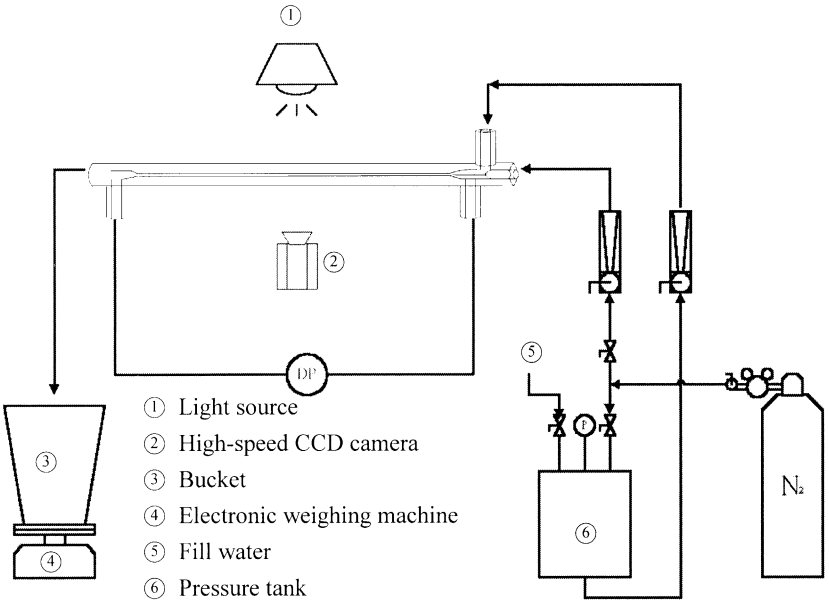

Fig. 1. A schematic diagram of the experimental loop.

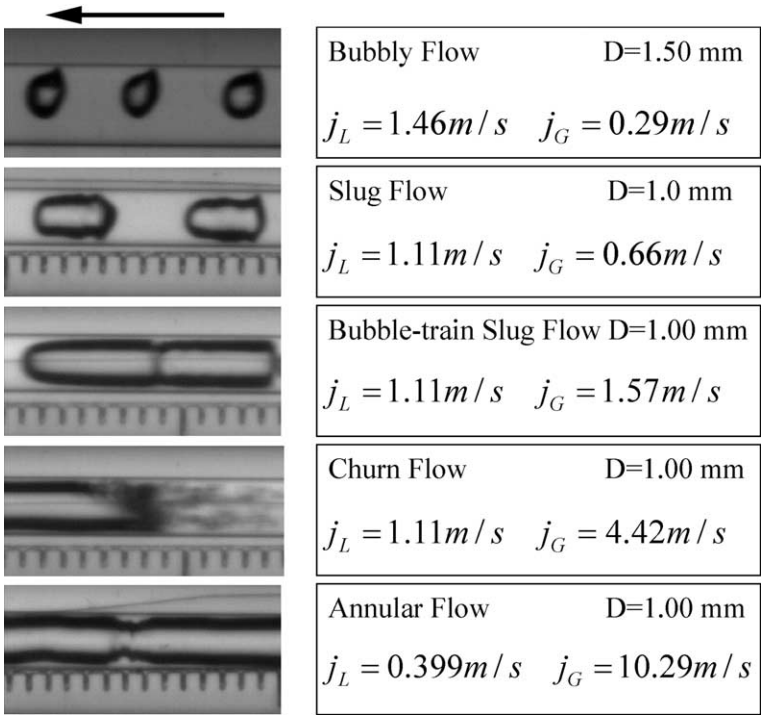

Fig. 2. Representative photographs of flow patterns in 1.5 and 1.0 mm horizontal tubes.

scattering. The incident light deflects at the vapor–liquid interface. As a result, the vapor–liquid interface appears to be dark (Hsieh et al., 1997).

The bubble velocity is of significant interest for understanding the two-phase flow mechanisms in micro-channels. In the present study the bubble velocity was measured by counting the number of frames for a particular bubble passing through a certain distance within the observation domain. A self-made ruler with minimum division of 0.5 mm was attached to the outer wall of the test section to accurately measure the distance traveled by the bubble in a time interval, as shown in Fig. 2. The velocities of 20 randomly selected bubbles were measured and averaged to obtain the mean velocity for each case of given gas and liquid superficial velocities in the slug, bubble-train slug and churn flow regimes. The standard deviation of velocity for those 20 randomly selected bubbles is usually below 5% of their mean values. For some of the bubble-train slug and churn flows, the standard deviations could be as high as 10–16% of their mean values.

3. Results and discussion

3.1. Two-phase flow patterns

Bubbly flow, slug flow, bubble-train slug flow, churn flow and annular flow could be identified in the present study for both horizontal and vertical flows. Fig. 2 displays the typical flow patterns

for horizontal flows. Bubbly flow could only be observed in the channels with the diameter of 1.5 mm in the present study. The gas rotameter in the present study does not allow such a low superficial velocity in the 1.00 mm diameter test section. Possibly caused by the effect of the buoyancy force, it can be seen that the bubbles flow in the upper half of the channel. For the channel with 1 mm diameter, the flow patterns for vertical flows under the conditions of same gas and liquid superficial velocities are quite similar to that for horizontal flows. This indicates that the predominance of the surface tension force in micro-channels of this size. Indeed, the Eotos number, defined as ratio of the buoyancy force to the surface tension force,

$$Eo = \frac{(\rho_L - \rho_G)gD^2}{\sigma} \tag{1}$$

is 0.134 under the room temperature conditions indicating that the surface tension force is much larger than the buoyancy force. Also caused by the capillary effect, no stratified flow was observed in the micro-channels of this study.

The slug flow, which is characterized by the existence of elongated bubbles, is very common at low gas superficial velocities in the present study. Due to the significant difference in the interfacial curvature at the front and the rear menisci of the bubble, the bubble–liquid–film interface is rippled unlike those observed in large size channels. For an elongated bubble in the micro-channel, the inside pressure may be assumed to be uniform, while the liquid pressure near the front meniscus is much smaller than that near the rear one as the bubble moves forward very fast. Consequently, the radius of the curvature for the front meniscus is much smaller than that in the rear one (Bretherton, 1961) and a rippled interface is resulted as shown in the figure. Moreover, there is usually no small bubble in the liquid film, between the Taylor bubble and tube wall, or in the liquid slug. This is quite different from that in large channels.

Under the earth gravity condition, the presence of bubble-train slug flow is unique in micro-channels. For this particular flow pattern, typically two to four bubbles, and possibly up to 10 or more, are in contact, like a train, with a clear interface between the connecting bubbles. The number of bubbles in a "train" seems to appear in a random manner. Fukano and Kariyasaki (1993) and Mishima and Hibiki (1996) have also reported the presence of such a bubble-train slug flow in their micro-channel experiments, but both groups did not characterize this flow pattern and did not distinguish it from the regular slug flow. On the contrary, such a flow pattern was not reported in the works of Tripplett et al. (1999a,b) and Coleman and Garimella (1999).

It is also interesting to note that such a peculiar flow pattern also appears in a large channel under the micro-gravity conditions (Zhao and Rezkallah, 1993). They named it as the frothy slug flow. The existence of the interface or "membrane" between two fast moving bubbles in contact is fascinating. Though the inertial force of the second bubble is large enough to overcome surface tension and break through the liquid slug (Zhao and Rezkallah, 1993) to coalesce together, it is still small to rupture the interface. Indeed, the Weber number based on the bubble inertial force, i.e.,

$$We = \frac{\rho_G D_H u_B^2}{\sigma} \tag{2}$$

of the order of unity indicates that the bubble inertial force is as high as the surface tension.

The features of the bubble-train slug flows in micro-channels under earth gravity and in large channels under the micro-gravity condition is not the same. For both situations, the gravity and so buoyancy force is negligibly small comparing with the surface tension force. Zhao and Rezkallah also adopted $We = 1$ as the criterion for the flow pattern transition from the slug flow to the bubble-train slug flow. However, the randomness of bubble number in a train deserves a more detailed investigation, as is provided in Section 3.2.

Churn flow is formed when the gas superficial velocity is large enough for the bubbles to rupture the membrane after breaking through the liquid slug between them. Furthermore, at this stage, the relative velocity between the bubbles and the liquid film is so high that the interfacial waves or ripples may be formed near the bubble tail; and some of the gas is entrained as tiny bubbles behind the large Taylor bubble. In fact, the cloud formed by the tiny bubbles appears very much like a comet tail.

At low liquid superficial velocities, if the gas superficial velocity is high enough, the annular flow pattern is formed. As in large channels, this flow pattern is characterized by the gas flow in the central part of the channel, while the liquid flows along the wall as liquid film. Interfacial waves with relatively large amplitudes wave observed. However, unlike that in large channels, droplet entrainment was seldom found.

Fig. 3 displays the flow pattern maps obtained in the present study for the 1.00 mm diameter test sections, respectively. The map, in general, agrees well with those reported by Fukano and Kariyasaki (1993) and Triplett et al. (1999a). However, Triplett et al. (1999a) did not report the bubble-train slug flow pattern; on the other hand, we fail to identify the slug–annular flow regime between slug and annular flow.

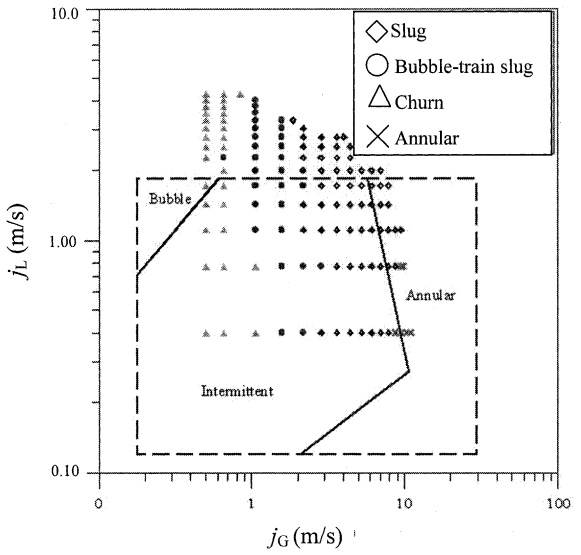

Fig. 3. Flow pattern map of 1.00 mm diameter channel and compared with that of Fukano and Kariyasaki (1993).

3.2. Bubble-train slug flow

The uniqueness of the bubble-train slug flow in the micro-channels deserves a more detailed investigation. The number of bubbles in a train appears in a random manner. The bar charts in Fig. 4 illustrates the time variations of the number of connecting bubbles of each train for several different cases, which is approximately corresponding to the time elapsed after the start of the video recording. It can be seen that the distribution of bubble numbers is quite random. As is

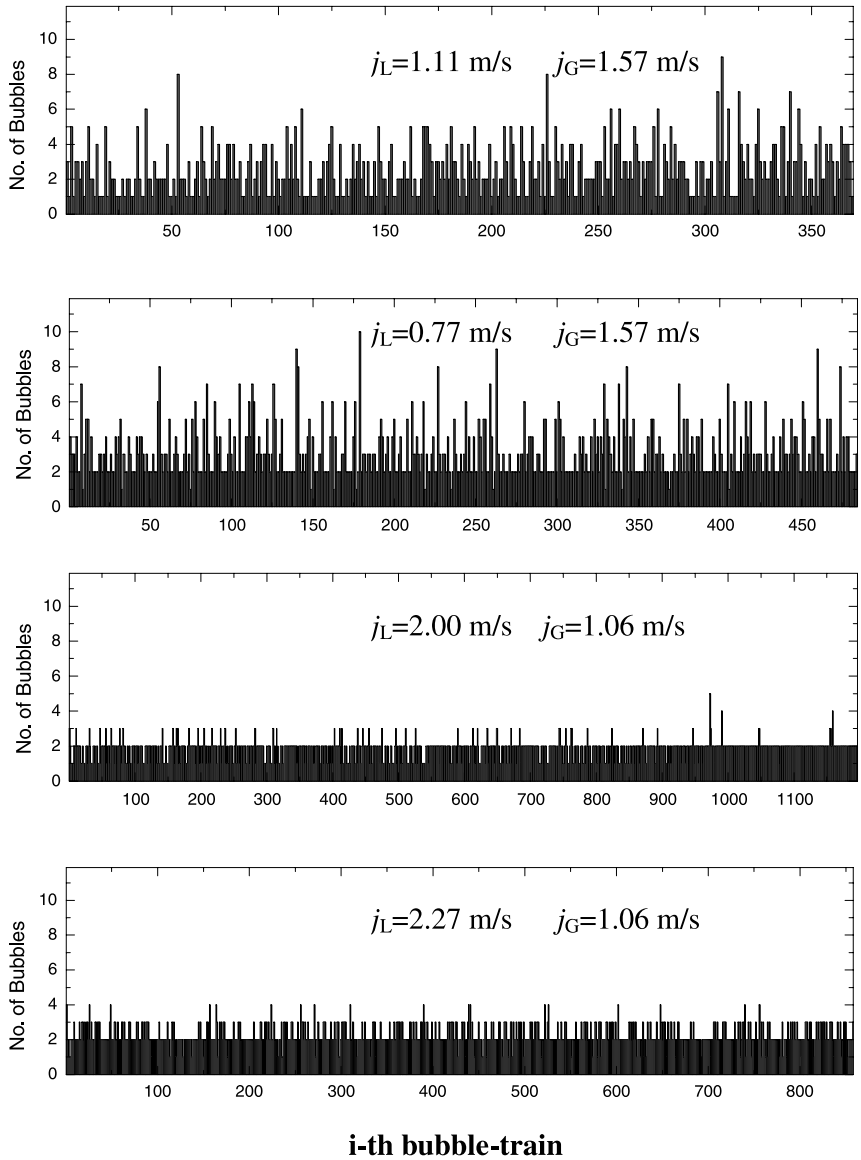

Fig. 4. Number of bubbles in bubble-train for each train in sequence for four selected cases.

pointed out previously, to form the interface between two fast moving bubbles, the inertial force of the second bubble must be large enough to overcome surface tension and break through the liquid slug to link together but should be small enough to keep the interface. It has been shown recently that a strong mixing effect is present in the liquid slug, in which the liquid near the capillary axis is moving forward, while the liquid near the wall is moving backward (Thulasidas et al., 1997). The interaction between the mixing flow in the liquid slug and the penetrating bubble would create a very complicated situation. Therefore, the formation of bubble-trains with random distribution of bubble number would be very possible. Moreover, it may also be speculated that the two-phase flow in the capillary is turbulent influencing the formation of bubble-trains with equal number of bubbles. In the present study, the bubble-train slug flow appears in 1-mm channel with liquid Reynolds number (Re_L), based on the liquid superficial velocity ranging from 440 to 4400. Although Re_L is not very large enough to induce turbulent flow for the liquid-only flows in the capillary, the presence of the bubble-train may very likely disturb the liquid flow and lead to the turbulence, especially for large Reynolds numbers. Fig. 4 suggests that the number of bubble in a train decrease with increase in liquid superficial velocities. This may be due to the strong mixing effect in the liquid slug at high liquid superficial velocities. The strong mixing effect in the liquid slug prevents the formation of trains with a large number of bubbles.

It is also interesting to examine the number-fraction distribution of bubbles in a train. Fig. 5(a) exhibits the number-fraction distribution as a function of liquid superficial velocity (j_L) for a low gas superficial velocity (j_G) of 1.06 m/s. The figure clearly indicates that for the low gas velocity, most of the bubble-trains consist of two connecting bubbles. For the cases of the small gas superficial velocity, the bubble velocity would be also relatively small and difficult to break through the liquid slug to form trains with many bubbles. Except for $j_L = 1.11$ and 2.78 m/s, the percentage of two-bubble trains ranges from 54% to 68%, 1 to 26% for single-bubble trains, i.e., separated bubbles, 5–30% for three-bubble trains, 0–6% for four bubble trains. There is no train with bubbles greater than 5. For $j_L = 1.11$ m/s, the distribution curve moves to the right and the most dominant train is that with three bubbles, which contributes about 42%. This unusual behavior at $j_L = 1.11$ m/s reflects again the random and unpredictable nature of the bubble-train slug flow. For $j_L = 2.78$ m/s, the single-bubble trains contribute most with 49%, the two-bubble trains come the next with 48% and the rest are three-bubble trains. It seems that a large liquid flow rate tends to hinder the formation of multiple-bubble trains at $j_G = 1.06$ m/s. As discussed

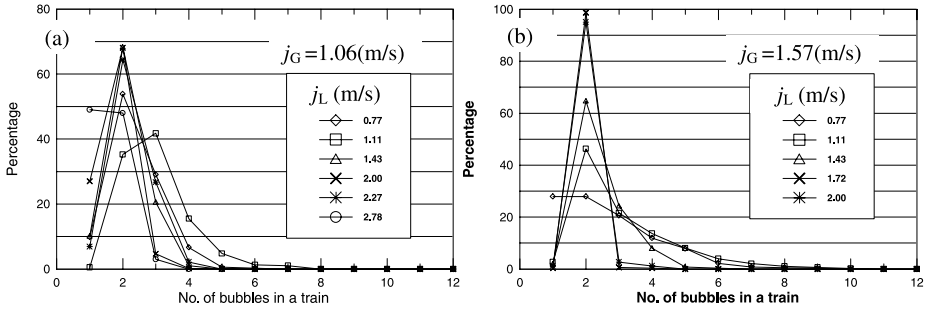

Fig. 5. Effect of liquid superficial velocity on number-fraction distribution of bubbles in a bubble-train for j_G equal to (a) 1.06 and (b) 1.57 m/s.

previously, the strong mixing effect at high liquid velocities hinders the formation of train with many bubbles. However, Fig. 5(b) does not show a consistent trend of liquid flow rate effect on the contributions of single-bubble train. This is another indication of the random nature of the bubble-train slug flow.

Conversely, single-bubbles dominantly appear only at the lowest liquid flow rate for the case of $j_G = 1.57$ m/s as shown in Fig. 5(b). That is, for $j_L = 0.77$ m/s, the single-bubble and two-bubble trains appear with an equal percentage of 28. For this particular case, three- or more-bubble trains appear less frequently. For $j_L > 0.77$ m/s, appearance of single-bubble train is almost negligible and two-bubble trains are mostly observed. For $j_L = 2.00$ and 1.72 m/s, the contribution of two-bubble trains is as high as 95% and 98%, respectively.

3.3. Bubble velocity

Two different approaches have been proposed to correlate bubble velocity in the literature. The first one correlates the relative velocity between the bubble and the mixture as a function of capillary number (Ca). For example, earlier experimental study of Fairbrother and Stubbs reported that (Thulasidas et al., 1995)

$$W = \frac{u_B - j_L}{u_B} = 1.0Ca^{1/2} \quad 7.5 \times 10^{-5} < Ca < 0.014, \tag{3}$$

where $Ca = \mu_l u_B/\sigma$ and u_B is bubble speed and μ_l is the liquid viscosity. Recently, Thulasidas et al. (1995) repeated their work in the same way for $0.003 < Ca < 1$. The second approach is similar to the drift flux model, which is widely used in the studies of large channel, to correlate the bubble velocity with the mixture volumetric flux. For example, Fukano and Kariyasaki (1993) reported that for their data with 1 mm test section

$$u_B = 1.21j^{1.05}, \tag{4}$$

while Mishima and Hibiki (1996) found that

$$u_B = 1.09j \tag{5}$$

for the test sections with diameters of 1.05 and 4.08 mm. In Eqs. (4) and (5) j is the superficial velocity of the two-phase mixture, i.e., the mixture volumetric flux.

In the present study, it is found that the relative velocity between the bubbles and the mixture volumetric flux is not only a function of Capillary number (Ca) but also a function of the liquid superficial velocity as shown in Fig. 6. For a given liquid superficial velocity, the relationship between W and Ca follows the trend that reported by Thulasidas et al. (1995). Another approach is, therefore, needed.

A correlation similar to the drift flux model is shown in Fig. 7. The figure clearly indicates that the bubble velocity can be correlated very well with the mixture volumetric flux for various different flow patterns as

$$u_B = C_0 j + u_{Gj}, \tag{6}$$

where C_0 is the distribution parameter and u_{Gj} is the drift velocity. The distribution parameter, C_0, is 1.017, 1.062 and 1.133 for slug, bubble-train slug and churn flow, respectively. On the other

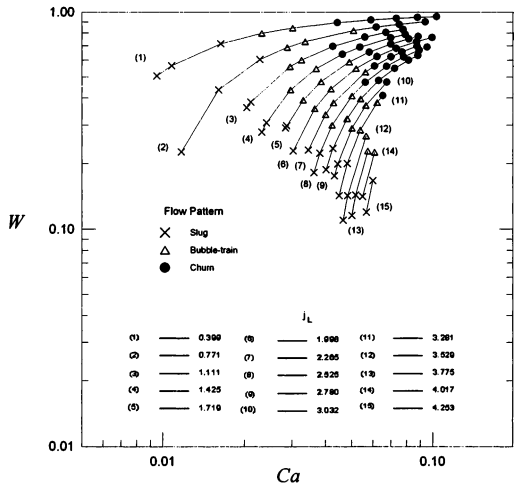

Fig. 6. The relation between W and Ca in 1.00 mm tube.

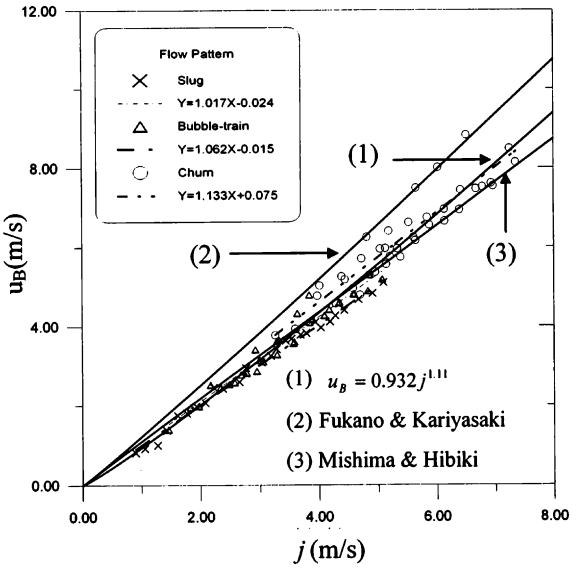

Fig. 7. Correlations for bubble velocity similar to the drift flux model.

hand, the "drift velocity" is −0.024 m/s (<3% of the minimum bubble velocity) for the slug flow, −0.015 m/s (<0.75% of the minimum bubble velocity) for the bubble-train slug flow, 0.075 m/s (<3% of the minimum bubble velocity) for the churn flow. The non-zero drift velocity is well within the measurement uncertainty, i.e., 5–16% depending on the flow regime. For each of the three flow patterns studied, the drift velocity may be treated as zero, as should be in a micro-channel (Bretherton, 1961).

For the data of all the three flow patterns, the bubble velocity can be correlated well with the mixture volumetric flux as

$$u_B = 0.932 j^{1.11}. \tag{7}$$

This approach is similar to that of Fukano and Kariyasaki, i.e., Eq. (4). Fig. 7 also illustrates a comparison of Eq. (7) with the correlations of Fukana/Kariyasaki and Mishima/Hibiki. The bubble velocity predicted by the correlation of Fukano and Kariyasaki is significantly higher than that predicted by Eq. (7), while Mishima and Hibiki's correlation underestimates the churn flow data of the present study.

3.4. Void fraction

The void fraction is also an important parameter in gas–liquid two-phase flows. In the 1 mm diameter micro-channel investigated in this study, bubbles other than the large Taylor bubble rarely appears, except for the churn flow. The bubble velocity may be treated approximately as the gas velocity. Thus, the average void fraction may be indirectly evaluated by the following fundamental equation:

$$\alpha = \frac{j_G}{u_G} = \frac{j_G}{u_B}. \tag{8}$$

Fig. 8 displays the void fraction as a function of gas and liquid superficial velocities. The void fraction increased monotonously with increasing of j_G at a given value of j_L. However, for the cases of $j_L = 0.399$ and 0.771 m/s, void fraction increased very rapidly with j_G until they reach their peak values, at which the flow pattern starts to change from bubble-train slug flow to churn flow for the case of $j_L = 0.399$ m/s. And then the void fraction, in general, decreases with in-

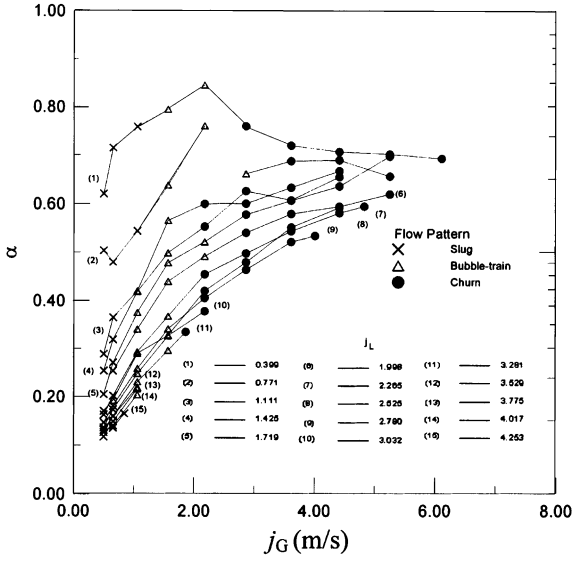

Fig. 8. Void fraction as a function of j_G and j_L.

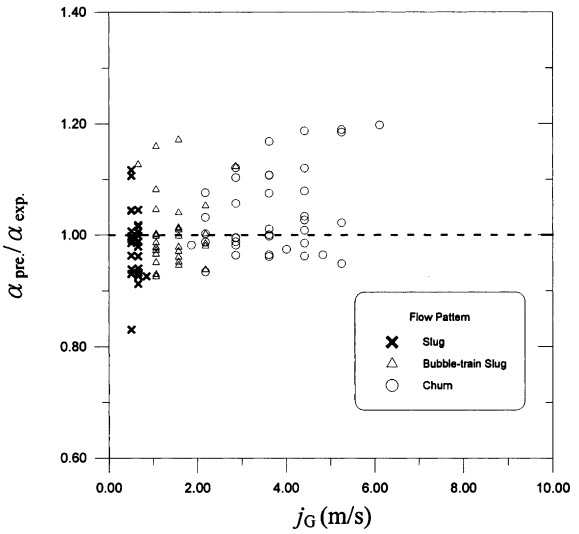

Fig. 9. Comparison of modified drift flux model prediction with void fraction data.

creasing j_G. This unusual trend is caused by that the slip ratio between the gas and liquid phase may also increase with increasing j_G.

Fig. 9 shows the comparison of the void fractions between the measured data and the modified drift flux model predictions based on the bubble velocity evaluated by Eq. (7), i.e.,

$$\alpha = \frac{j_G}{0.932 j^{1.11}}. \tag{9}$$

The figure shows that Eq. (9) predicts the data within 20% for all three flow regimes. The deviation is found to be as high as 40% if the homogeneous flow model, which assumes the zero slip between the gas and liquid phase, is adopted.

4. Summary and conclusions

The present study investigates experimentally nitrogen–water two-phase flow in glass microchannels with diameters of 1.00 and 1.50 mm. The gas and liquid superficial velocities were ranged from 0.502 to 11.0 m/s and from 0.399 to 3.53 m/s, respectively. Visualization of two-phase flow pattern in the channels was made possible by using a high-speed digital camera. Bubbly flow, slug flow, bubble-train slug flow, churn flow and annular flow could be identified for both horizontal and vertical flows. The following conclusions may be drawn from the present study:

1. Due to the predominance of surface tension over buoyancy force in a micro-channel, a peculiar flow pattern called bubble-train slug flow is present. Such a flow pattern is characterized by the presence of bubble-train formed by several bubbles connecting together with a membrane between two neighboring bubbles. Such a flow pattern is also found in large channel under microgravity conditions as reported in the literature.

2. The number of bubbles in a bubble-train appears in an irregular manner indicating its inherent turbulent nature. Most of the bubble trains consist of two to three connecting bubbles, though those with more than 10 bubbles can also be found. A large liquid flow rate tends to hinder the formation of trains with many bubbles connecting together.
3. The relative velocity between the bubbles and the superficial liquid velocity is not only a function of capillary number based on the bubble velocity, as was proposed in some previous studies, but also a function of liquid superficial velocity. On the other hand, the bubble velocity can be correlated well by a modified drift flux model for various different kinds of flow patterns.
4. The void fraction can be correlated well by an approach based on the modified drift flux model. The homogeneous flow model predictions poorly agree with the experimental data.

Acknowledgements

This work was supported by the National Science Council of Taiwan under the contract no. of NSC 89-2212-E-007-093. Mr. K.J. Shen's excellent work in conducting the statistics of bubble-train slug flow is highly appreciated.

References

Aligoodarz, M.R., Yan, Y., Kenning, D.B.R., 1998. Wall temperature and pressure variations during flow boiling in narrow channels, Heat transfer 1998. In: Proceedings of 11th IHTC, vol. 2, pp. 225–230.

Bretherton, F.P., 1961. The motion of long bubbles in tubes. J. Fluid Mech. 10, 166–188.

Coleman, J.W., Garimella, S., 1999. Characterization of two-phase flow patterns in small diameter round and rectangular tubes. Int. J. Heat Mass Trans. 42, 2869–2881.

Fukano, T., Kariyasaki, A., 1993. Characteristics of gas–liquid two-phase flow in a capillary tube. Nucl. Engng. Des. 141, 59–68.

Hsieh, C.C., Wang, S.B., Pan, C., 1997. Dynamic visualization of two-phase flow patterns in natural circulation loop. Int. J. Multiphase Flow 23, 1147–1170.

Kennedy, J.E., Roach Jr., G.M., Dowling, M.F., Abdel-Khalik, S.I., Ghiaasiaan, S.M., Jeter, S.M., Quershi, Z.H., 2000. The onset of flow instability in uniformly heated horizontal microchannels. J. Heat Trans. 122, 118–125.

Lin, S., Kew, P.A., Cornwell, K., 2001. Two-phase heat transfer to a refrigerant in a 1 mm diameter tube. Int. J. Refrig. 24, 51–56.

Mishima, K., Hibiki, T., 1996. Some characteristics of air–water two-phase flow in small diameter vertical tubes. Int. J. Multiphase Flow 22, 703–712.

Peng, X.F., Wang, B.X., 1993. Forced-convection and flow boiling heat transfer for liquid flow through microchannels. Int. J. Heat Mass Trans. 36, 3421–3427.

Thulasidas, T.C., Abraham, M.A., Cerro, R.L., 1995. Bubble-train flow in capillaries of circular and square cross section. Chem. Engng. Sci. 50, 183–199.

Thulasidas, T.C., Abraham, M.A., Cerro, R.L., 1997. Flow patterns in liquid slugs during bubble-train flow inside capillaries. Chem. Engng. Sci. 52, 2947–2962.

Triplett, K.A., Ghiaasiaan, S.M., Abdel-Khalik, S.I., Sadowski, D.L., 1999a. Gas–liquid two-phase flow in microchannels, Part I: two-phase flow pattern. Int. J. Multiphase Flow 25, 377–394.

Triplett, K.A., Ghiaasiaan, S.M., Abdel-Khalik, S.I., LeMouel, A., McCord, B.N., 1999b. Gas–liquid two-phase flow in microchannels, Part II: void fraction and pressure drop. Int. J. Multiphase Flow 25, 395–410.

Xu, J.L., Cheng, P., Zhao, T.S., 1999. Gas–Liquid two-phase flow regimes in rectangular channels with mini/micro-gaps. Int. J. Multiphase Flow 25, 411–432.

Zhang, L., Koo, J.M., Jiang, L., Banerjee, S.S., Ashegi, M., Goodson, K.E., Santiago, J.G., Kenny, T.W., 2000. Measurements and modeling of two-phase flow in microchannels with nearly-constant heat flux boundary conditions. In: Proc. Micro-Electro-Mechanical Systems (MEMS)-2000, vol. 2, pp. 129–135.

Zhao, L., Rezkallah, K.S., 1993. Gas–liquid flow patterns at microgravity conditions. Int. J. Multiphase Flow 19, 751–763.